Materials Science-Poland, Vol. 23, No. 3, 2005

Quantitative mapping of the elastic properties of electron-beam damaged silica-based low-*k* films

LE JIANG[1], H. GEISLER[2], E. ZSCHECH[2*]

[1]Gesellschaft für Wissens- und Technologietransfer der TU Dresden mbH,
Chemnitzer Strasse 48 b, D-01187 Dresden, Germany

[2]AMD Saxony LLC & Co. KG, Materials Analysis Department,
Wilschdorfer Landstrasse 101, D-01109 Dresden, Germany

A quantitative technique for mapping the elastic modulus, performed on organosilicate glass (OSG) thin films with different surface conditions, is described. This modulus mapping technique provides highly valuable information about the elastic properties at the near-surface region of the films. The results show that low-*k* films can be modified by electron beams, yielding a near-surface region with increased stiffness. Compared to quasi-static nanoindentation, the modulus mapping technique is more surface sensitive, and therefore has a better capability to detect slight differences in elastic properties between ultra-thin films of different thicknesses on top of OSG films.

Key words: *modulus mapping; nanoindentation; low*-k*; electron-beam damage; surface*

1. Introduction

Low-*k* dielectric materials for insulating thin films are needed to diminish power consumption and minimize the cross talk between on-chip metal interconnects in leading-edge microelectronic products [1, 2]. Electron treatments can be applied for the local densification of OSG materials in order to increase the stiffness of the backend-of-line (BEoL) layer stack. The local change of the chemical bonding of the interlayer dielectric (ILD) material, however, increases the effective permittivity (*k* value), and consequently the electrical performance of the Cu/low-*k* structure is influenced. It is an extremely challenging task to change the local electronic polarisability and the chemical bonding of the ILD material in such a way that the stiffness of the material is increased significantly and the effective *k* value is increased only slightly. In addition, the adhesion between the etch stop layer and low-*k* material should be improved. As the interconnect line spacing of ultra large scale integrated circuits continues to

[*]Corresponding author, e-mail: ehrenfried.zschech@amd.com

shrink, optimising the electrical performance of Cu/low-*k* structures and mechanical properties of BEoL layer stacks becomes increasingly important for the integration of low-*k* materials.

For the optimisation of ILD material properties, considering both the integral thin -film material and in particular the near-surface regions, with a typical extension of 10–100 nm, it is necessary to understand the relationship between changed electronic polarisability and chemical bonding, as well as between permittivity and modulus [3]. Particularly, the extent of damage has to be studied quantitatively. An additional argument for the need to understand electron–material interaction is the fact that the imaging of patterned OSG structures is challenging for electron microscopy since the structures are damaged during examination and shrinkage is observed. The analysis of several individual damage processes results in the conclusion that the radiation damage depends on the electron energy, and that it is proportional to the energy dose deposited in the sample for a certain electron energy [4]. The goal of this paper is to propose a methodology for evaluating and quantifying the extent of electron-induced modification in OSG thin films, based on changed nanomechanical properties. Near-surface mechanical properties are examined quantitatively by an elastic modulus mapping technique. This technique allows one to distinguish between ultra-thin layers of different thicknesses with a high surface sensitivity.

2. Experimental

In this study, a carbon-doped oxide dielectric material comprised of Si, C, O, and H (OSG, also called SiCOH), deposited on a blanket wafer using plasma-enhanced chemical vapour deposition (PECVD), was locally modified by the electron beam of a scanning electron microscope (SEM). The modified areas of the OSG film were investigated by applying the modulus mapping technique [5], implemented in a Tribo-Indenter nanomechanical testing instrument with in-situ scanning probe microscopy (SPM) imaging capability (Hysitron, Inc., Minneapolis, MN). A scheme of the Hysitron TriboIndenter measuring system is shown in Fig. 1. During the mapping process, the dynamic test is performed by oscillating the indenter tip with small forces while monitoring the resultant displacement and phase lag due to the material response. Simultaneously, SPM imaging allows the indenter tip to scan across the material surface. The system continuously monitors the stiffness of the sample and provides a plot of the stiffness as a function of the position on the sample. The stiffness is given at each pixel of the image, and the modulus can be calculated if the geometry of the probe tip is known. The complex modulus information obtained by this modulus mapping technique includes the real and imaginary parts, $E = E' + iE''$, and provides the storage (E') and loss (E'') characteristics of a material. The E' and E'' values are given by [6]

$$E' = \frac{k_s\sqrt{\pi}}{2\sqrt{A_c}} \tag{1a}$$

$$E'' = \frac{\omega C_s\sqrt{\pi}}{2\sqrt{A_c}} \tag{1b}$$

respectively, where k_s is the storage stiffness proportional to the ratio of the force and displacement, C_s is the loss stiffness proportional to the phase lag, ω is the frequency, and A_c represents the contact area calculated based on the radius of curvature of the probe tip.

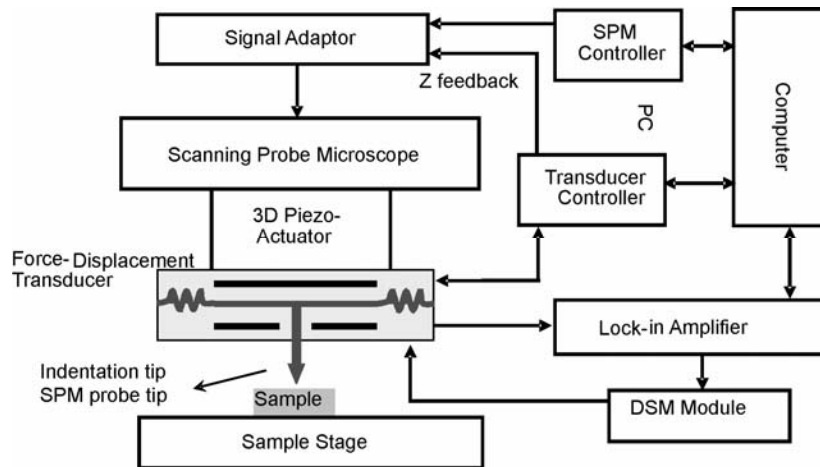

Fig. 1. Schematic diagram of the Hysitron TriboIndenter combined with the nanoDMA and SPM techniques. The DSM module provides the alternation of the signal configurations, necessary for quasi-static or dynamic testing

The results of such a modulus mapping are equivalent to a dynamic indentation test performed at each pixel in a 256 × 256 image. Areas with the size of about 9 µm × 7 µm in an unpatterned low-*k* OSG film with a thickness of about 1000 nm – the original value of *k* was 2.7 – were exposed to an electron beam in an SEM, applying electron beam energies of 1, 3, and 5 keV for the same exposure time. Using the modulus mapping technique, 15 µm × 15 µm areas were scanned with a Berkovich diamond tip mounted on the nanoindentation tool. The measuring parameters (e.g., the oscillation frequency of the ac-force – 200 Hz, dc-force – 2 µN, and amplitude of the ac-force – 1.5 µN) were identical for the as-deposited and electron-beam treated regions of the sample.

Quasi-static nanoindentation was carried out on the same samples for comparison with the modulus mapping technique. A schematic representation of load vs. displacement data for an indentation experiment is shown in Fig. 2 [7, 8]. As the indenter is first driven into the film, both elastic and plastic deformation occurs. After the indenter is withdrawn, the elastic displacements are recovered, and an analysis of the

elastic unloading data can then be used to experimentally relate the measured quantities to the projected contact area and elastic modulus. For any axisymmetric indenter, the relationship is

$$S = \frac{dP}{dh} = \frac{2}{\sqrt{\pi}} E_r \sqrt{A_c} \tag{2}$$

Here, $S = dP/dh$ is the experimentally measured stiffness of the upper portion of the unloading data and E_r is the reduced modulus given by

$$\frac{1}{E_r} = \frac{1-\nu^2}{E} + \frac{1-\nu_i^2}{E_i} \tag{3}$$

where E and ν are Young's modulus and Poisson's ratio for the specimen, respectively, and E_i and ν_i are the same quantities for the indenter.

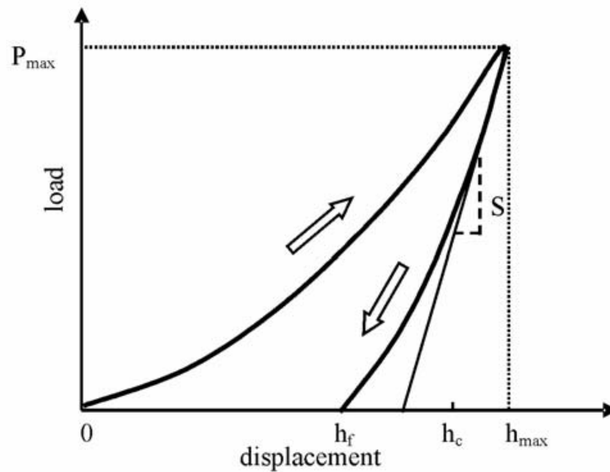

Fig. 2. A schematic representation of load vs. displacement data for an indentation experiment: $P_{\max}$ – the peak indentation load, $h_{\max}$ – the displacement at peak load, h_f – the final depth of the contact impression after unloading, h_c – the contact depth, S – the initial unloading stiffness

To evaluate the contact area at peak load during the nanoindentation of a thin film, special procedures are used to estimate the contact depth h_c from the load –displacement data, and the contact area is determined by evaluating the area function at this depth, i.e. $A_c = f(h_c)$. The most common procedure determines h_c as

$$h_c = h_{\max} - 0.75 \frac{P_{\max}}{S} \tag{4}$$

3. Results

For comparison of the modulus mapping technique with the quasi-static nanoindentation technique, OSG thin films 500 nm thick were capped with ultra-thin Ta films. The Ta film thickness varied between 10 and 30 nm. The elastic properties of these ultra-thin films, measured quantitatively by applying the modulus mapping technique, were compared with the data from measurements performed on identical samples applying the quasi-static depth-sensing nanoindentation technique with a normal force F_n ranging from 5 μN to 80 μN.

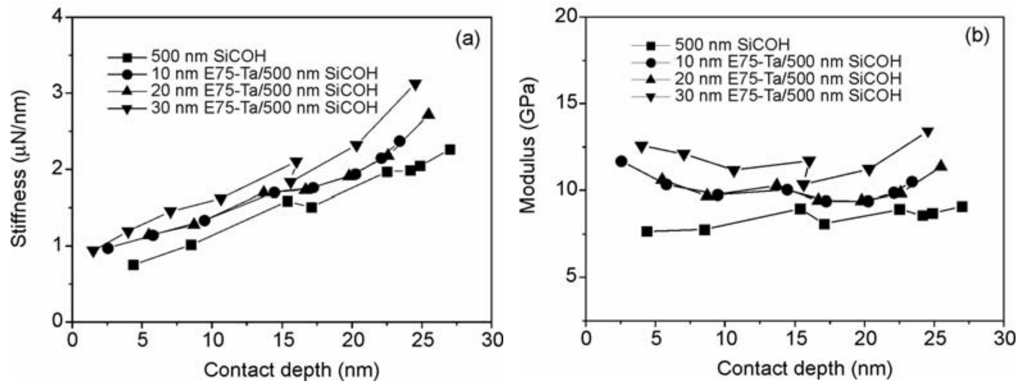

Fig. 3. Stiffness (a) and elastic modulus (b) vs. contact depth from quasi-static indents made on a pure OSG film and on ultra-thin Ta films with different thicknesses on top of OSG films

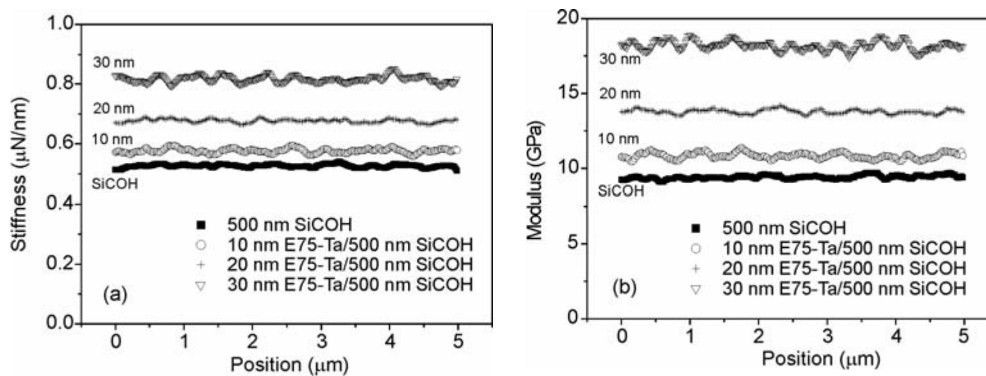

Fig. 4. Stiffness (a) and elastic modulus (b) cross-sectional data from stiffness and modulus maps of a pure OSG film and of ultra-thin Ta films with different thicknesses on top of OSG films

These forces cause shallow indents compared to the film thickness. The storage modulus is used to compare with the quasi-static nanoindentation results for a loss modulus of nearly zero, since the material shows small or negligible viscoelastic properties. As shorthand, the term modulus is used in what follows instead of reduced elastic modulus, which is usually measured by nanoindentation. As expected, both the

stiffness and modulus, obtained with quasi-static indentation and modulus mapping, are increased for the OSG/Ta thin film samples as compared to the bare OSG films. Both the indentation experiment and modulus mapping show an increase of the mechanical stiffness of the samples with increasing Ta film thickness (see Fig. 3 and 4). There is no significant difference between the stiffness and elastic modulus, however, for samples with 10 and 20 nm thick Ta films as seen by the quasi-static indentation technique, whereas a line-section analysis of the quantitative maps shows a clear difference in the stiffness and modulus of these two samples. Extracted from Fig. 4, the mean values of stiffness for a bare OSG film and for OSG films with 10 nm, 20 nm, and 30 nm ultra-thin Ta films on top are 0.53, 0.58, 0.68, and 0.82 μN/nm, and the respective values of elastic modulus are 9.5, 11, 14, and 18 GPa. These results are in agreement with the quasi-static indentation results calculated by extrapolating quasi-static indentation curves down to a contact depth of 1 or 2 nm.

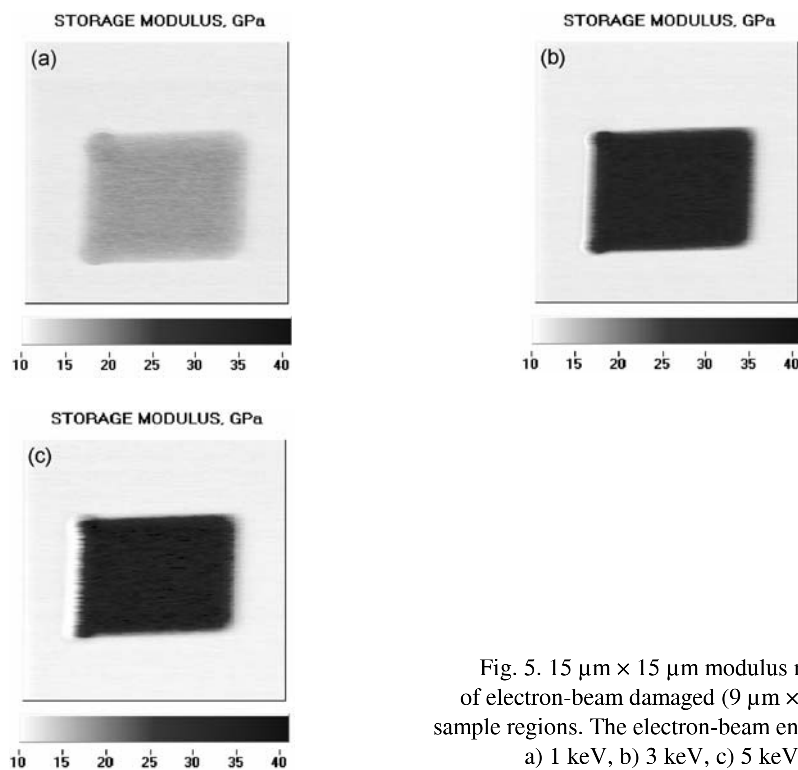

Fig. 5. 15 μm × 15 μm modulus maps of electron-beam damaged (9 μm × 7 μm) sample regions. The electron-beam energy was: a) 1 keV, b) 3 keV, c) 5 keV

Due to the local exposure of the surface to an electron beam, a shrinkage of the OSG thin film was observed. This shrinkage depends on the applied electron energy. Higher electron energies caused more serious damage, leading to deeper craters in the OSG film. Different image contrasts between the damaged region and as-deposited area are shown on quantitative modulus maps in Fig. 5.

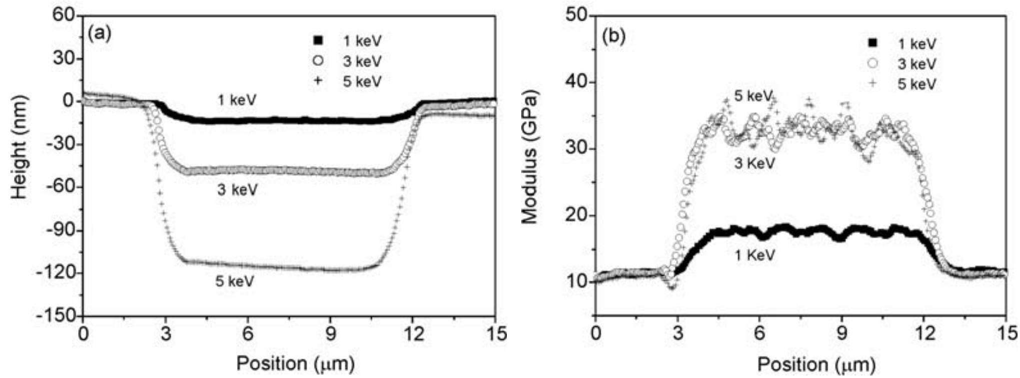

Fig. 6. Cross-sectional data from topography and modulus maps: a) the crater profile caused by the electron beam, b) cross-section profiles of the modulus maps in Fig. 5

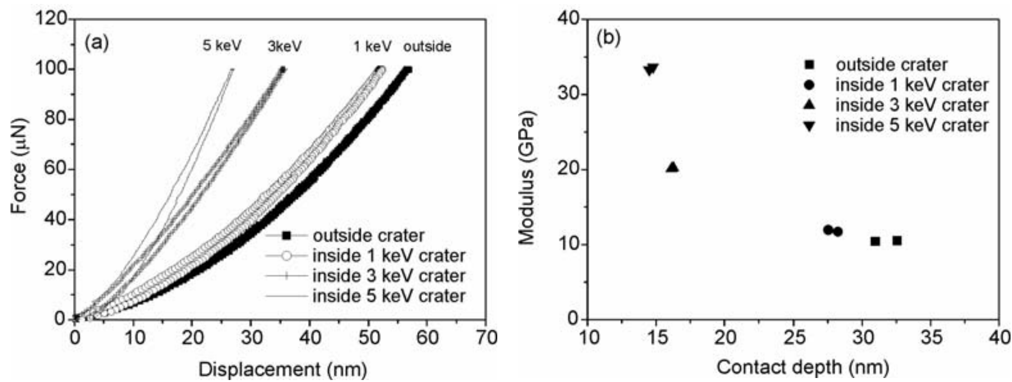

Fig. 7. Quasi-static indentation data for the electron-beam damaged regions of the OSG sample: a) force-displacement curves of samples locally exposed to electron beams of different energies (exposure time for all samples – 25 s), b) the calculated elastic modulus for the sample regions corresponding to the curves shown for in (a)

The crater depth was determined directly from line-section profiles of topography maps as represented in Fig. 6a. The mean values of the storage modulus, determined from a line-section analysis of the modulus maps, are 11, 17, 32, and 35 GPa for 0, 1, 3, and 5 keV electron beam energies used in the surface treatment, respectively (Fig. 6b). The more damaged OSG film regions are characterized by steeper force-displacement curves, and thus, by higher modulus values. This result is confirmed by the quasi-static indentation data shown in Fig. 7a. The modulus values of OSG films are 10.5 GPa, 12 GPa, 20 Gpa, and 33 GPa in the case without damage and with damage with 1 keV, 3 keV, and 5 keV electron beam energies, respectively (Fig. 7b). The mapping data for the as-deposited film and for the area with 5 keV electron beam treatment are comparable with the quasi-static indentation data but those for areas damaged with 1 keV and 3 keV electron beams are higher than the values obtained from indents made on the same sample.

4. Discussion

It is necessary to note that the elastic modulus obtained from quasi-static indentation depends on the stiffness of the material which is determined by the slope of the unloading curve, using a power-law fit to the initial unloading data, and by the area function of the indentation probe based on Pharr–Oliver theory [7]. At very shallow penetration depths, the accuracy of the tip area function becomes more critical for the calculation of the elastic modulus. Using the currently defined area function at very small contact depths (less than 10 nm), the modulus decreases with increasing contact depth. This decrease probably results from the indentation size and the strain gradient plasticity effect [9, 10], which is a near-surface effect. After reaching a minimum value, the modulus increases with increasing depth due to the constraint of the stiffer substrate. Considering that the maximum penetration depth of the tip is about 3.5 nm for the modulus mapping method and that the contact depth is even lower in this case, it is reasonable that the mapping technique results in higher modulus and lower stiffness values, approaching values from low-depth quasi-static indentations.

As expected, the OSG film was modified to different degrees when exposed locally to electron beams for the same exposure time with different energies. The larger the electron beam energy, the more serious the damage on the OSG material, i.e., the deeper were the craters. Since the degree of damage varies with depth for a single crater, higher modulus mapping results for 1 keV and 3 keV electron-beam damaged samples as compared to quasi-static indentation results for the same samples can be explained by the different information depths and surface sensitivities of these techniques. Only the very near-surface region is analysed with the modulus mapping technique, while the quasi-static indentation method measures film properties over a larger depth range. For example, the maximum penetration depth for quasi-static indentation in a crater formed by a 1 keV electron beam is 50 nm, whereas the maximum penetration depth of modulus mapping is only about 3.5 nm. This difference in depth sensitivity explains the different modulus values. In the case of the crater formed by a 5 keV electron beam, the depth of the crater is about 120 nm, and both methods provide similar results. A supposed explanation for this result is that the damage is nearly the same at positions 25 nm and 3.5 nm deep for a material damaged with a 5 keV electron beam energy.

Since the modulus mapping technique is more surface sensitive than quasi-static indentation, it is possible to detect slight differences in the elastic properties of ultra-thin layers on top of OSG films. It should also be noted that with the quasi-static indentation method the data from very shallow indents could be significantly affected by measuring noise, drift, or tip area function, which all cause errors. Therefore, the modulus mapping technique should be applied for determining the elastic properties of thin films and near-surface regions.

5. Conclusion

In summary, we have shown that modulus mapping is a valid method for assessing the process-induced modification of dielectric materials, such as OSG damage caused by electron-beam treatment. The modulus mapping technique implemented in a nano-indentation tool with in-situ SPM imaging capability allows a mapping of the stiffness and elastic modulus quantitatively on the scale of a few micrometers on low-*k* films with a very high surface sensitivity. Consequently, the extent of damage caused by a specific process step can be quantified with high spatial resolution. Small areas on low-*k* films, which were locally exposed to an electron beam in a SEM, showed distinct image contrast, the electron-beam treated regions being stiffer than the regions not treated. Different electron energies and/or exposure times lead to quantitatively different modulus maps. The modulus values resulting from the maps agree well with low-load quasi-static nanoindentation data. Small changes in the modulus can be resolved, as shown for different surface treatments of OSG films. Our results show that modulus mapping is more surface sensitive than quasi-static indentation. Modified near-surface regions of low-*k* films can be characterized, and ultra-thin layers can be distinguished quantitatively.

Acknowledgements

Valuable discussions with Dmytro Chumakov and sample preparation performed by Petra Hofmann, both with AMD Saxony, Dresden, Germany, are gratefully acknowledged. The authors would like to thank Reinhard Sturm and Henry Urban, GWT Dresden, Germany, for supporting this study.

References

[1] MAEX K., BAKLANOV M.R., SHAMIRYAN D., IACOPI F., BRONGERSMA S.H., YANOVITSKAYA Z.S., J. Appl. Phys., 93 (2003), 8793.
[2] HO P.S., [in:] *Materials for Information Technology*, E. Zschech, C. Whelan, T. Mikolajick (Eds.), Springer, Berlin, in press (2005).
[3] IACOPI F., TRAVALY Y., STUCCHI M., STRUYF H., PEETERS S., JONCKHEERE R., LEUNISSEN L.H.A., TOKEI ZS., SUTCLIFFE V., RICHARD O., VAN HOVE M., MAEX K., Mat. Res. Soc. Symp. Proc., Warrendale/PA, 812 (2004), 19.
[4] EGERTON R.F., LI P., MALAC M., Micron, 35 (2004), 399.
[5] WARREN O.L, WYROBEK T.J., Meas. Sci. Technol., 16 (2005), 100.
[6] Hysitron Incorporated, *NanoDMA for Viscoelastic Materials*, available online at: http://www.hysitron.com/Products/Sellsheets/new_nanoDMA.htm
[7] OLIVER W.C., PHARR G.M., J. Mater. Res.. 7 (1992), 1564.
[8] PHARR G.M., OLIVER W.C., MRS Bulletin, 17 (1992), 28.
[9] NIX W.D, GAO H., J. Mech. Phys. Solids, 46 (1998), 411.
[10] SAHA R., XUE Z.Y.,.HUANG Y, NIX W.D., J. Mech. Phys. Solids, 49 (2001), 1997.

Received 11 June 2005
Revised 4 August 2005